Computational Modeling of Wet Deck Slam Loads with Reference to Sea Trials

Michael R. Davis[1] , James R Whelan[2] and Giles A Thomas[3]
[1]University of Tasmania, Hobart, Australia 7001
[2]INTEC Engineering Pty.Ltd. Level 2, 190 St. George's Terrace, Perth, WA 6000, Australia
[3]Australian Maritime College, Launceston, Tasmania 7250

ABSTRACT

Wave piercing catamarans exhibit a particular form of wet deck bow slam with the maximum loading arising at the top of the arched cross section between the centre bow and outboard hulls. We consider here the modelling of these slams by means of drop testing of a two dimensional model of the vessel cross section near the bow where slams are known to occur. In addition to physical modeling, loads predicted by a vertical momentum balance for the cross section are considered. The conditions and variation of entry speed of the drop test model were selected so as to correspond to observations for typical slam events observed in full scale vessel trials. It is found that the two dimensional representations of the slam entry load exceeds the largest slam which has so far been observed in sea trials by a factor of about three. This difference is attributed to the three dimensional nature of the full scale slam event which is not constrained by two dimensional motion conditions. It is proposed that the vertical momentum method be applied in ship motion and loading computations with a correction factor to reduce predicted loads so as to better correlate with observed maximum slam loading.

1 INTRODUCTION

Holloway and Davis (2006) have demonstrated the capabilities of the time domain solution of the high speed ship motion problem. The method gives very accurate prediction of wave response over a wide range of encountered wave frequency, vessel speed and sea direction when compared with measured test data for a variety of designs (Davis and Holloway, 2003a,b). The method readily incorporates multi-hull configurations, encounter with oblique seas and the effect of ride control systems. In the present paper we will consider methods for incorporating slam events into time domain motion and loads solutions.

Wet deck slams associated with the impact of a rising water surface with the wet deck of a catamaran can cause significant structural damage (Thomas et al, 2001) and there is a need to include slam events in computations of global loads. In the case of a wave piercing catamaran with small main hulls near the bow and with a centre bow above the waterline to protect against deck diving in following seas, the hull cross section in the bow region is of a double arch form. This gives rise to a particular type of slam at the stage when the arch fills and venting of air within the arch ceases. The purpose of this investigation is to develop a computational model which gives an adequate representation of the consequent slam forces for the purpose of global load calculations during a slam event. Giannotti (1975) observed that the most critical portion of a catamaran for hydrodynamic impact occurrence is the bottom of the transverse structure (that is the wetdeck) where slamming may cause damage to the local panels and buckle of the ship frames. Slamming also induces a dynamic whipping response in the vessel structure (Thomas et al 2001) and may accelerate fatigue failures of the hull.

Cook (1998) conducted trials of an 8m research catamaran, finding that slam loads were substantially higher and of much shorter duration than the underlying wave loads. Haugen and Faltinsen (1999) undertook full-scale measurements of the wetdeck slamming of a 30m catamaran. Large vertical accelerations with substantial whipping motions were observed during wetdeck slam events and were compared with a theoretical hydroelastic model. It was found that wetdeck slamming may occur in sea states well below the operational limits given by the DNV rules. The normal relative velocity between the wetdeck and water surface determined the maximum induced load. Steinman, Fach and Menon (1999) found that responses resulting from slam events consisted of an initial response followed by a backlash stress, which may be larger than the initial stress response, a local structural response and then a global modal response. The extent of each of these responses was dependent on the location relative to the location of the slam impact. Roberts, Watson and Davis (1997) analysed slam events for 81m and 86m INCAT wave piercing catamarans and found that the maximum stress was highest in a 2m significant wave height sea even though the vessel had operated in waves with height of up to 10m. This was attributed to the operator reducing speed in adverse conditions. The vertical acceleration at the LCG was found to increase only slowly with wave height and speed reduction by the operator also influenced this trend. Large slamming loads were found to be significantly larger than regular wave loads. Yakimoff (1997) used a finite element model and full-scale trials of an 81m INCAT wave piecer and found that 66% of the fatigue damage suffered by the vessel was due to slamming and the subsequent dynamic response. Roberts and Yakimoff (1998) developed global design loads for an 86m INCAT wave piercing catamaran using finite element models and full-scale data for transient loads induced due by the slamming of the centre bow and wetdeck. Thomas, Davis, Holloway and Roberts (2003b) measured the slamming response of a 96m INCAT wavepiercer and developed a definition of a slam based on the time rate change of the strain transients. The relationships between maximum slam stress and significant wave height, slam occurrence frequency, slam Froude number and vessel Froude number were determined from the data records. The whipping response of the vessel to slamming was also examined. During the trials a severe slam event occurred which caused damage to the vessel and a slam load of 10,060kN was calculated using the structural finite element analysis. The bending moment and the shear force exceeded the DNV sag rule predictions. Thomas et al (2003a) reported on the sea trials of an INCAT 86m catamaran and found the trends for the 96m vessel were similar to those of the 86m vessel.

Drop testing of two and three-dimensional models into water is the principal experimental method for investigating the water entry process. The model geometries for which previous experimentation has been published include rigid vee wedges, elastic vee wedges, rigid three-dimensional wedges with forward speed, rigid and elastic flat plates, cylinder models, a range of realistic hull forms, cones, spheres, highly elastic models and parabolic panels. The entry of two-dimensional rigid wedges into water has been investigated for various deadrise angles by Kreps (1943) and Bisplinghoff and Doherty (1952). Accelerations were recorded and high-speed photography was used to investigate the deformation of the free surface during impact. These tests were used to validate the added mass theories of Kreps (1943), Wagner (1932), Mayo (1952), von Karman (1929) and Bisplinghoff and Doherty (1952). The added mass calculated by Kreps (1943) was greater than the added masses determined from experiment, whilst the theory of von Karman (1929) yielded added masses which were slightly too low for deadrise angles greater than 10^{o}. The other four methods over estimated the added mass for deadrise angles less than 15^{o} but under estimated for deadrise angles greater than 35^{o}. Hayman, Haug and Valsgård (1991) discussed the difficulties involved in measuring surface pressures because the peak values were of very short duration. Stavovy and Chuang (1976) tested entry of three-dimensional rigid vee wedges with forward speed at a range of forward speeds and found that peak pressure initially increases with impact angle until a maximum was obtained at approximately 3^{o}. The experimental results compared well with the theory of Wagner (1932) and Chuang (1969). The impact pressure was found to be approximately 100 times greater than the planing pressure. It was concluded that the relative normal velocity was the most significant in determining the peak pressure during impact. Radev and Beukelman (1992) also measured the peak pressures and rise time of pressure at forward speed. The peak values of the slamming pressure were proportional to the square of the vertical impact speed but with a significant forward speed effect. Payne (1981) reviewed added mass theories for the wedge entry problem and concluded that the approach of von Karman (1929) was both simple and adequate. Real slam events will depend significantly on the precise detail of the way in which the hull and water surface meet and also on the effects air venting and of residual air in the top of the arched cross section. For that reason the aim of the present work is restricted to the establishment of relatively straightforward basis for computational modelling of overall loads and does not seek to quantify the precise nature of localised panel pressures. Against this background it was considered that a modified added mass method is most likely to give an adequate representation of global slam loads, since it will correctly simulate the overall vertical momentum balances involved in a slam event. However, it is necessary to consider also the effect of entrained air in the top of the wet deck arches in the case of a wave piercing catamaran bow cross section.

2 SLAM LOADS OBSERVED IN SEA TRIALS

Given the complexity of a bow area wet deck slam for a wave piercing catamaran, reference is first made here to the results of sea trials observations of large slam events.

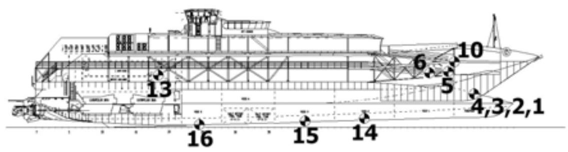

Figure 1 INCAT 96m wave piercing catamaran showing strain gauge locations

These have been reported by Thomas et al (2003a, 2003b). Figure 1 shows the location of strain gauges on an INCAT 96m wave piercer type vessel. Figure 2 shows an example of the strain gauge time records during an extreme slam event on this vessel. Two slams are evident at an interval of approximately 5 seconds, the first being approximately twice the severity of the second.

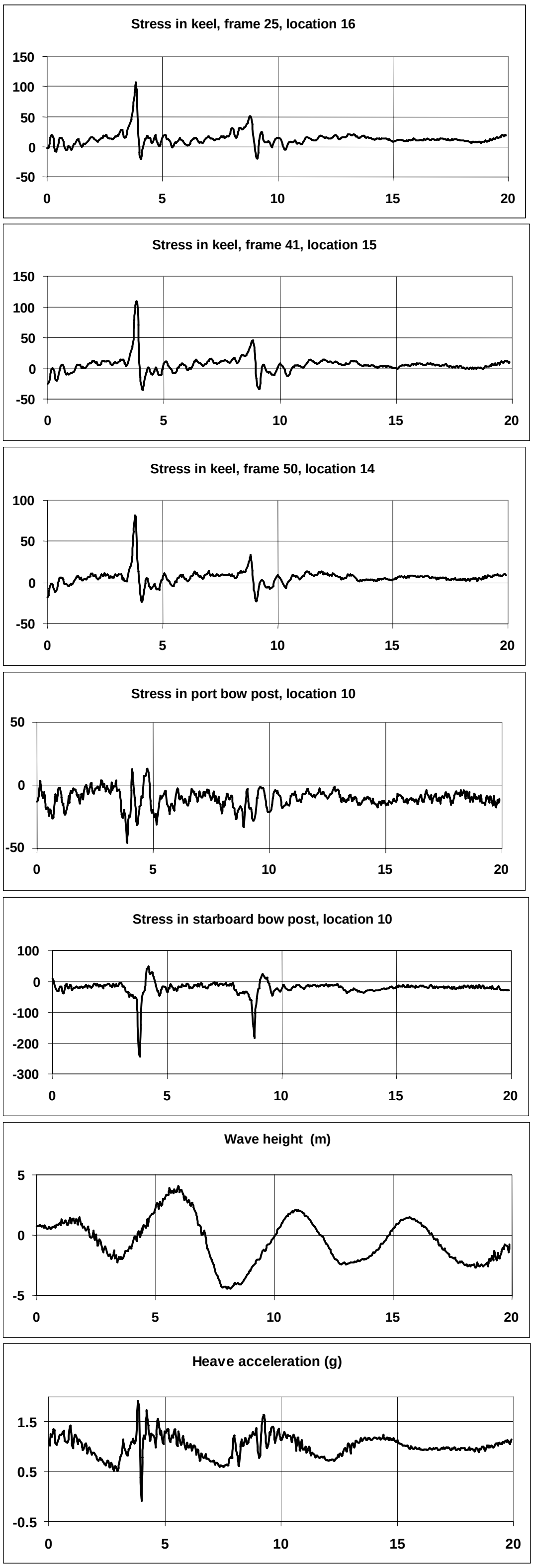

Figure 2 Record of very large slam event, 19 knots speed, INCAT 96m vessel (Abscissa: seconds; ordinate: MPa). Gauge locations as in figure 1.

Otherwise the two slams appear generally similar and we see that the time records along the keel (upper three traces of figure 2) indicate generally similar stress levels at the three positions: gauge 16 (at frame 25, 63.4m from the bow), gauge 15 (at frame 41, 44.1m from the bow) and gauge 14 (at frame 50, 33.0m from the bow). We see that there is strong transient bending along the length of the hull. In the case of these very large slams there is not strong evidence of whipping after the slam. This may be because for these very large slams the bow enters the water deeply and remains submerged for sufficient time that whipping is suppressed by the damping action of the water around the bow surfaces. The dominant peak stress is the initial tension in the keel corresponding to upward bending of the hull. The stress responses in the vertical internal bow posts at location 10 on figure 1 show that the slam is strongly concentrated on the starboard side of the vessel since there is relatively little slam induced stress in the port post. The starboard post shows a strong compressive stress as would be expected. It appears that the slam was concentrated on the starboard side of the bow at the top of the arched cross section between the centre bow and the main starboard demi-hull. The vessel was fitted with a TSK wave radar mounted on the centre bow sensing the distance to the instantaneous water surface and a co-located accelerometer. The signals from these enabled the time variation of water surface height and the distance from the centre bow keel to the water surface to be computed and the sixth trace in figure 2 shows the profile of water surface beneath the bow. Both slams give maximum load as the water surface is rising beneath the bow as would be expected. Finally the vertical heave acceleration at the vessel centre of gravity (final trace in figure 2) also shows evidence of the slam event and some evidence of whipping, but these transient motion responses at the LCG are not very large being comparable to the general vertical acceleration in encountered waves without slamming. Clearly the duration of the slam is sufficiently short that there is no substantial global motion response due to the slam. The distance between the centre bow keel and the instantaneous water surface is shown in figure 3 during the first very large slam event. It is seen that the centre bow keel penetrates 6m into the water in this case over a total entry time of about 1.3 seconds. This profile of the entry process is to be used here as the basis for modelling the entry event during a model drop test. In particular we calculated the ratio of the vertical velocity of the hull relative to the water surface at the instant that the top of the arch intersects the average water surface to the maximum initial velocity just prior to the slam event. This ratio is used as a dimensionless parameter to be simulated during model drop tests.

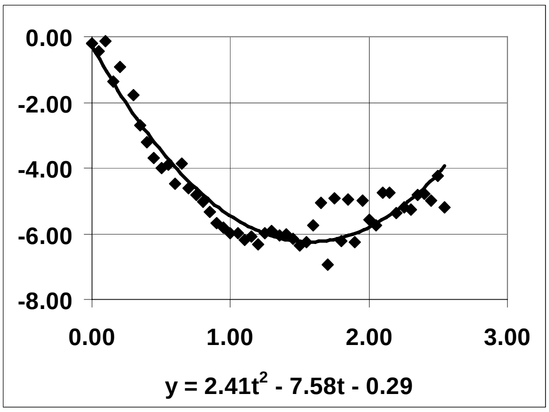

Figure 3 Variation of separation (m) between centre bow keelat frame 59 and undisturbed wave surface with time (s) during large slam event

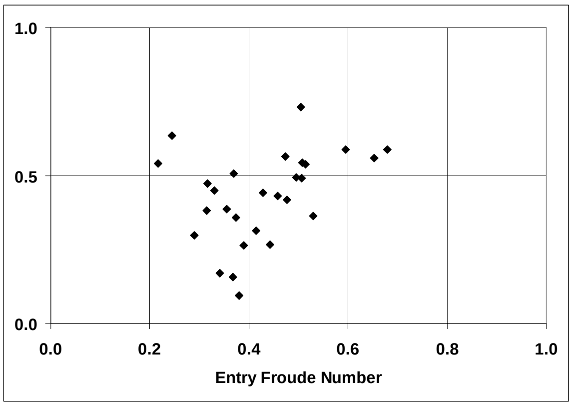

Figure 4 Ratio of velocity when arch top passes the undisturbed water level to velocity when demihull keels pass undisturbed water level for slams observed in sea trials of 98m INCAT vessel

Values of the velocity ratio are shown in figure 4 for a number of slams observed during the sea trials. The overall range is between 0.1 and 0.7. Thomas (2003) has taken the maximum stress values observed at all the strain gauges fitted to the vessel and reconciled these with finite element analysis (using the NASTRAN package and a 64000 element FE model of the ship structure) of the vessel subjected to vertical loads under the bow area. The loading was adjusted in terms of peak value, location of the peak and distribution about the peak until there was best agreement between the observed peak stresses and those computed by the FEA. The results are shown in figure 5, the maximum loading being about 0.3 MPa, the entire slam load in this case being on the starboard side of the vessel centreline. Figure 6 shows the maximum slam loads calculated in a similar manner for six slams: we see that the extreme slam event gave a maximum load of approximately 1600 tonnes. This greatly exceeded the trendline for the other slams which were analysed, which were representative of

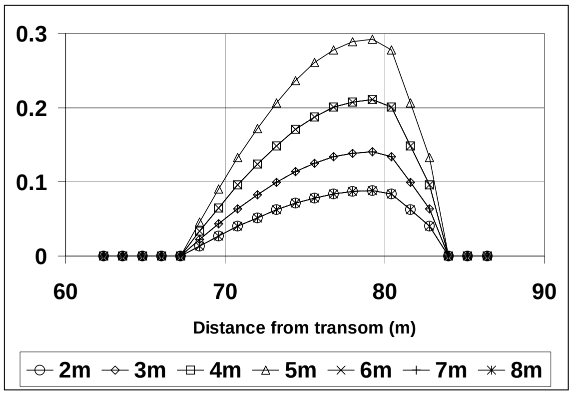

Figure 5 Distribution of slam loading under centre bow starboard arch during very large slam event on INCAT 98m vessel (Mpa, legend indicates distance from vessel centreline).

what might be termed more usual slamming, and indicates the potential for occasional extreme events to occur depending on the precise form of the water surface as it meets the underside of the hull. Large slam loads would be expected if the rising water surface is relatively smooth and conforms closely to the hull surface. Indeed it is not certain that the very large slam observed represents the extreme of what is possible and the only way in which that could be resolved is to make observations of large numbers of slams. However the very large slam recorded here does exceed the more usual slam loads by a factor of about three and on that basis does appear to have been a relatively extreme event and gave rise to structural damage.

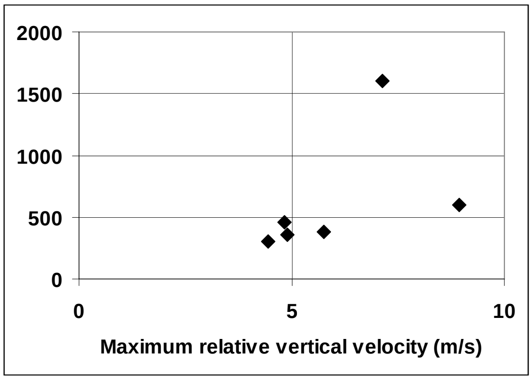

Figure 6 Variation of computed slam maximum upward load (tonnes) on bow with water relative entry velocity for INCAT 96m vessel.

3 MODEL DROP TESTS OF THE SLAM PROCESS

Two-dimensional modelling has been carried out by various authors to provide a basis for predicting slam loading. This modellling has either been by use of scale physical models or by boundary element computational fluid dynamics, generally on a frictionless basis. The main issue with such modelling, whether physical or computational, is whether the two dimensional constraint and generally smooth initial water surface gives rise to much larger loads than occur in practice with an irregular water surface and a significantly three dimensional interaction. A two dimensional model of the cross section of the INCAT wave piercing design at the position of maximum slam loading was constructed and tested by dropping into smooth water. The main parameters which can be controlled in such tests are the drop height, which simply defines the maximum velocity just prior to water entry, and the mass of the model. In the present work the drop height parameters were selected so as to simulate the maximum entry Froude number. The model drop height H (the distance between the top of the arch and the water surface at the point of model release into free fall) also has to be selected to represent the full-scale conditions in terms of the maximum entry velocity. Full scale trials data (such as that shown in figure 3) indicated the entry Froude number $Fr_e = V_s / \sqrt{gB} = \sqrt{2H / B}$, based on the maximum vertical relative velocity prior to the slam event between hull and water. This translates to a requirement for H/B to lie in the range 0.3 to 0.7 approximately.

The model mass was selected so as to represent the velocity ratio observed in the full scale sea trials as shown in figure 4. A large model mass tends to increase this ratio towards unit value since a very massive model maintains its velocity during interaction with the water to a greater extent than a very light model, which slows more rapidly. The required model mass was calculated using a vertical momentum balance of the type first used by von Karman (1929), the added mass of a hull section in the water being represented by a semicircle based on the maximum beam of the section. In this case the added mass of the center bow and the demi-hulls increases as the section enters the water and then undergoes a rapid increase as the arch is filled completely after which the added mass is based on the waterline beam of the whole vessel cross section. Application of a vertical momentum balance thus gives:

$$(M_h + \sum_i \rho\pi b_i^2 / 8)V = M_h V_1 \qquad (1)$$

where M_h is the model hull mass per unit length, ρ is the water density, b_i is the waterline beam of hull i, V is the downward velocity of the model at any instant and V_1 is the model velocity at the instant that the keel enters the water. For the slam which occurs as the arches between the hulls fill we have:

$$(M_h + \sum_i \rho\pi b_i^2 / 8)V_s = (M_h + \rho\pi B^2 / 8)V_2 \qquad (2)$$

where B is the overall beam of the model, V_s is the velocity just before the slam and V_2 the velocity just after the slam. This gives the ratio of minimum velocity after the slam V_2 to the maximum velocity V_1 as

$$V_2 / V_1 = \frac{M_h}{M_h + \rho\pi B^2 / 8} = \frac{1}{1 + \pi / 8m*} \qquad (3)$$

where m* is the mass ratio of the model. In order to simulate a velocity ratio in the range 0.2 to 0.6 a model mass parameter of m*=0.1 to 0.58 is required.

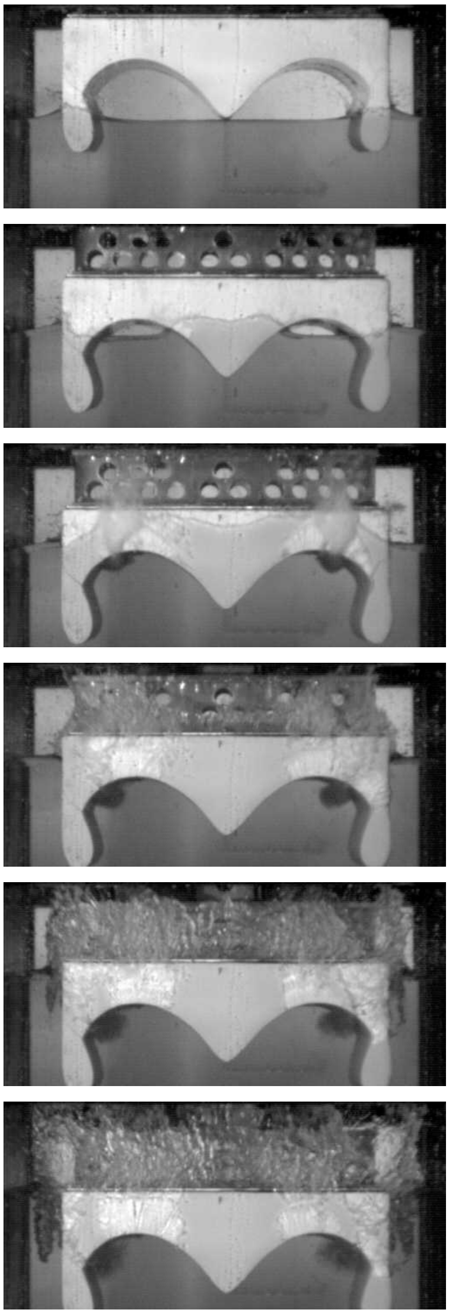

Figure 7 Drop test of INCAT section model (photos at 50, 100, 120,140,160 and 180 ms after deemihull keel touches water surface, m*=0.29, H/B=0.37)

Figure 7 shows a high speed photographic sequence of a drop test of the 544mm wide model into initially still water in a two dimensional test tank with m*=0.29. There was a small clearance between the two dimensional model flat end faces and the transparent ends of the tank through which the photographs were taken. It was calculated that this clearance was sufficient to allow the air within the top of the model arches to vent freely as the model entered the water. It was found that the clearance between the transparent end wall of the tank and the model face if varied did not significantly alter the rates of deceleration of the model. Nor did it affect the observed pressures at the mid point of the model between the tank wall (the model was 350mm long so the pressure tappings were 175 mm from the end walls). This venting simulates well the entry of a three dimensional vessel bow where air would not be fully enclosed by the hull surfaces and the water and so woulde free to vent in a lengthwise direction during a full scale slam.

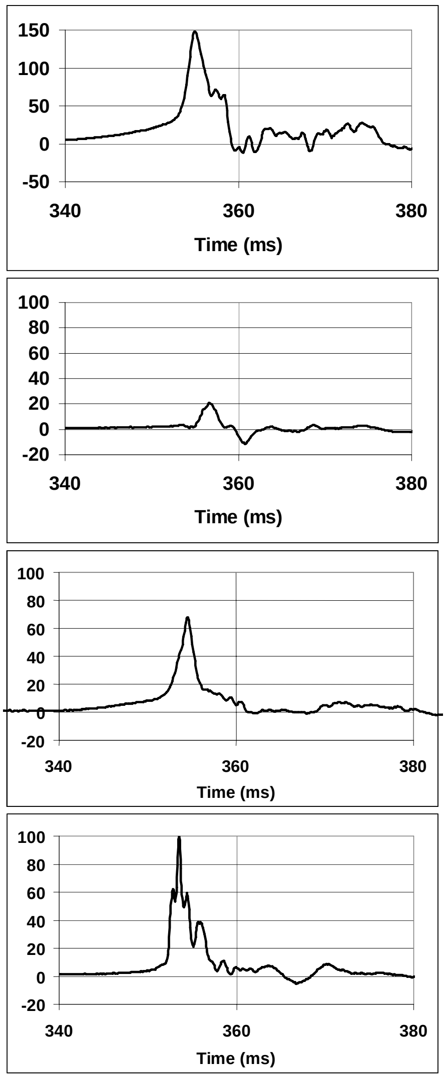

Figure 8 Transient records during water entry of INCAT model (as in figure 7). Top: acceleration (m/s^2). Lower three figures: Pressure (kPa) at positions 52.5mm, 149mm (arch top) and 199mm from centreline (model width is 544mm). Time of drop release=140ms.

When the quantity of air in the arch became quite small it tended to break up into bubbles and thus became entrained in the water and not fee to vent due to the resistance of the bubbles to motion through the water. The remaining entrapped air bubbles can be seen as a cloud at the top of the arch at 120 ms (third photo of the sequence). It can then be seen that the entrapped air bubbles act as a marker of water motion, and reveal that the water sweeps around the top of the arch towards the outboard end of the arch. As has been discussed by Whelan et al (2003) this motion has a beneficial effect in alleviating the maximum slam pressures and is a consequence of having a relatively voluminous centre bow with the top of the arch well away from the vessel centreline.

Transient acceleration and pressure records during a typical drop test are shown in figure 8. We see clearly that the maximum pressures occur near to the top of the arch and of course correspond to the time of maximum upward acceleration which reaches a value of about 15g for the test model. Close to the centreline the maximum pressures are relatively small (figure 8, second record from top) and the maximum pressure increases becoming highest beyond the top of the arch (figure 8, lower record shown). This result is consistent with observations of vessels in service where slight deformation of hull panels outboard of the top of the arch has sometimes been observed due to wave impact. It can also be seen that the pressure maximum occurs slightly later in time near to the centre line. Whilst this region enters the water first it seems that the pressure rise is due to the transmission of a pressure wave from the point of arch closure near the top of the arch rather than being due to the initial water entry. The maximum acceleration occurs at about the same time that there is a very large pressure maximum near the top of the arch.

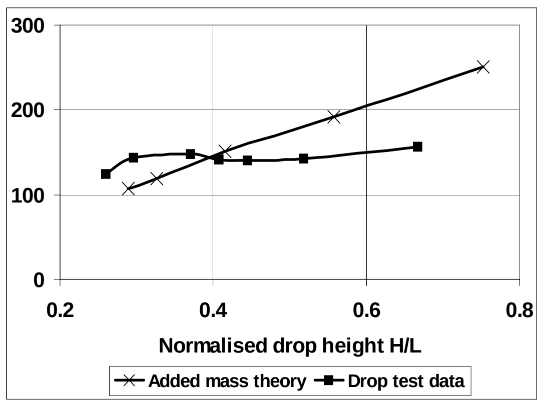

Figure 9 Comparison of maximum acceleration measured in drop tests with added mass momentum analysis (Ordinate: Maximum acceleration, m/s^2) (INCAT model, m*=0.29)

Figure 9 compares the variation of maximum acceleration observed during the drop tests with that predicted by the vertical momentum balance in terms of the initial vertical momentum of the test model and the added mass of the water. Whilst the experimental results are in general agreement with the momentum balance, we see that the momentum theory predicts a more rapid rise in maximum acceleration with normalised drop height. It would appear that there is a variation of effective added mass with drop height (ie with vertical entry velocity), this most likely being due to a reduction of added mass for lower entry velocities as might be expected. Figure 10 shows the variation of ratio of the velocity at the point when the arch top passes the undisturbed water line to the maximum entry velocity as the central keel first enters the water. As would be expected the model with the smaller mass number shows a greater reduction of velocity. The progressive reduction of the minimum relative velocity once again indicates that for the larger drop heights and entry velocity the effective added mass is higher.

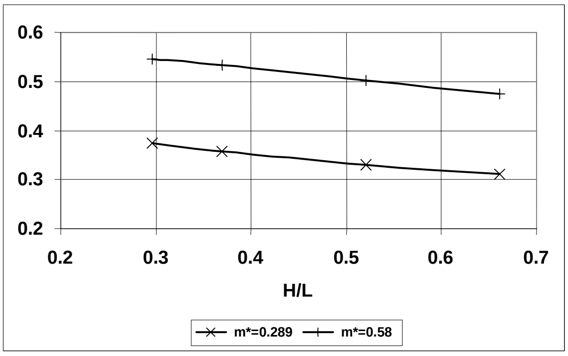

Figure 10 Ratio of velocity when arch top passes undisturbed water level to velocity at demihull keel entry in model drop tests.

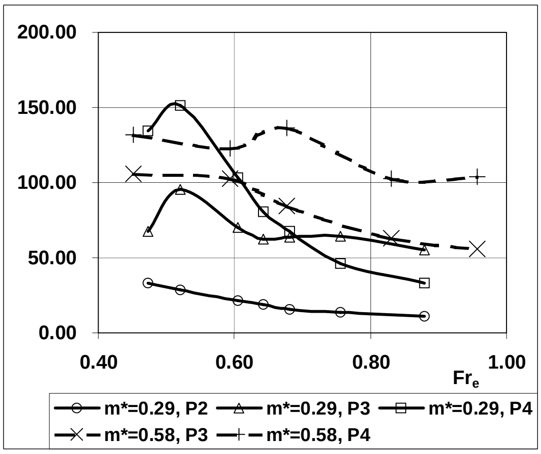

Figure 11 Variation of maximum pressure coefficient with entry Froude number in model drop tests of INCAT section

If the maximum pressures are normalised in terms of the dynamic pressure defined in terms of the vertical relative velocity, $C_{p\max} = p_{\max} / \rho V_s^2$ then we find that the calculated pressure coefficients are very large, as shown in figure 11. This is a consequence of the constraint arising from the arch closure process and the associated transverse movement of displaced water. The largest value arise near to the top of the arch of course and also for the model with the larger mass which retains a higher velocity during water entry and so generates larger maximum pressures. The maximum force coefficient defined on the basis of the entry velocity as $C_{F\max} = F_{\max} / \rho B V_s^2$ where F_{max} is the maximum force per unit length on the model, determined from the maximum acceleration. Values of C_F are shown in figure 12 and this parameter is also seen to give quite large values of course. The model with the greater mass also experiences the largest force maximum since it retains a higher velocity during the entry process and so produces more severe slams.

4 CONCLUDING DISCUSSION

The maximum force coefficient results obtained in the model drop tests can be extrapolated to full-scale vessel conditions on the basis of the maximum force on the cross section per unit length of hull. We can thus compare the maximum loads observed during the sea trials with those observed in the drop tests. The data record for the very large slam event on INCAT hull 042 shows that simulation of this particular extreme event would require a model mass ratio m*= 0.1 and a normalised drop height H/B=0.1. We find by extrapolating from the results of figure 12 a full scale maximum slam force of 7609kN/m is predicted. The maximum slam force per unit length calculated from the full scale trials strain gauge records and finite element analysis was only 31% of this value. This shows that the two dimensional drop test loads exceed the full-scale loads by about a factor of three. It seems from this outcome that the two dimensional constraint is severe and that three-dimensional effects ameliorate the maximum loads on a complete vessel. It seems therefore that if maximum slam loads are to be realistically predicted for a moving vessel in a seaway then this must be done on the basis of three-dimensional modelling. This could be physical or computational, or else on an ad hoc basis on the basis of loads observed during sea trials. It will be rather unrealistic to attempt to apply two-dimensional computations to the prediction of absolute slam loads. Nevertheless, two dimensional modelling can be useful in a more general sense, as was concluded by Whelan et al (2003) in respect of the finding the best sectional design to minimise slam loadings by moving the top of the arch as far outboard as practicable.

5 ACKNOWLEDGEMENT

The support of INCAT Tasmania, Revolution Design Pty Ltd, the Australian Research Council and the University of Tasmania is gratefully acknowledged.

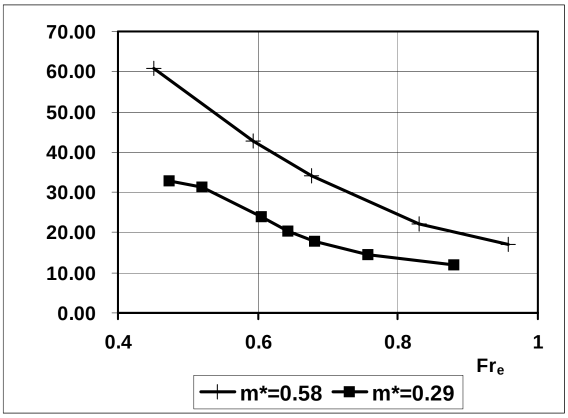

Figure 12 Variation of maximum force coefficient measured during model drop tests with entry Froude Number Fr_e.

REFERENCES

Bisplinghoff, R.L and Doherty, C.S. (1952). Some studies of the impact of vee wedges on a water surface. Journal of the Franklin Institute, **253**, 547-561.

Cook, S. (1998) Investigation into wave loads on catamarans. Proceedings Australian Maritime Engineering Conference AME98, Sydney.

Chuang, S-L. (1969) Theoretical investigations on slamming of cone-shaped bodies. Journal of Ship Research, **13**, 276-283.

Davis, M. R. and Holloway, D.S. (2003a). The influence of hull form on the motion of high speed vessels in head seas, Ocean Engineering, **30**, 2091-2155.

Davis, M. R. and Holloway, D. S. (2003b). Motion and passenger discomfort on high speed catamarans in oblique seas, International Shipbuilding Progress, **50**(4), 333-370, 2003b.

Giannotti, J. (1975). Prediction of slamming loads for catamarans, Seventh Annual Offshore Technology Conference, Houston, Paper OTC2281, 348-357.

Haugen, E. M. and Faltinsen, O. (1999). Theoretical studies of wet deck slamming and comparisons with fullscale measurements. Proceedings FAST 99 5th International Conference on Fast Sea Transportation, Seattle, 577-591.

Hayman, B., Haug, T., and Valsgård, S. (1991). Response of fast craft hull structures to slamming loads. Proceedings FAST 91 First International Conference on Fast Sea Transportation, Trondheim, 381-398.

Holloway. D. S. and Davis, M. R. (2006). Ship motion computations using a high Froude number time domain strip theory, Journal of Ship Research, **50**(1).

R. L. Kreps. (1943). Experimental investigation of impact in landing on water. National Advisory Committee for Aeronautics, Technical Memorandum 1046,.

Mayo, W. L. (1952). Hydrodynamic impact of a system with a single elastic mode I-theory and generalised solution with an application to an elastic airframe. National Advisory Committee for Aeronautics, Technical Report No. 1074.

Payne, P. (1981). The vertical impact of a wedge on a fluid. Ocean Engineering, **8**(4), 421-436.

Radev, D. and Beukelman, W. (1992). Slamming on forced oscillating wedges at forward speed part 1 – test results. International Shipbuilding Progress, **39**(420), 399-422.

Roberts, T. J., Watson, N. L., Davis, M. R. (1997). Evaluation of sea loads in high speed catamarans. Proceedings of FAST97 4th International Conference on Fast Sea Transportation, Sydney, 311-316.

Roberts, T. and Yakimoff, P. (1998). Adequate global design loads for fast ferry vessels. Proceedings of 14th Fast Ferry International Conference.

Steinmann, P., Fach, K. and Menon, B. (1999). Global and slamming sea loads acting on an 86m high speed catamaran ferry. Proceedings of FAST99 5th International Conference on Fast Sea Transportation, Seattle, 709-718.

Stavovy, B. and Chuang, S-L. (1976). Analytical determination of slamming pressures for high-speed vehicles in waves. Journal of Ship Research, **20**(4), 190-196.

Thomas, G.A. (2003). Wave slam response of large high speed catamarans. University of Tasmania, PhD thesis.

Thomas, G. A., Davis , M. R., Whelan, J. L. and Roberts, T. J. (2001). Slamming response of large high speed catamarans. Proceedings of FAST2001, 6th International Conference on Fast Sea Transportation, Southampton.

Thomas, G. A., Davis, M. R., Holloway, D. S. and Roberts, T. J. (2003a). Transient dynamic slam response of large high-speed catamarans, Proceedings of FAST2003 7th International Conference on Fast Sea Transportation, 2(B1):1-8, Naples.

Thomas, G. A., Davis, M. R., Holloway, D. S., Watson, N. L. and Roberts, T. J. (2003b). The slamming response of a large high speed catamaran, Marine Technology, **40**(2):126-140., von Karman, T. (1929). The impact on seaplane floats during landing. National Advisory Committee for Aeronautics, Technical Report TN 321.

Wagner, H. (1932). The phenomena of impact and planing on water. National Advisory Committee for Aeronautics, translation 1366, , Washington, D.C.

Whelan, J.R., Holloway, D.S., Davis, M. R. and Roberts, T.J. (2003) Wetdeck slamming of high speed catamarans with a centre bow, Proceedings of FAST 03 7th International Conference on Fast Sea Transportation, Vol 2(B1), 33-40, Naples, 7-10.

Yakimoff, P. (1997) State-of-the-art computer simulation for structural analysis of high speed catamarans. Proceedings of FAST97 4th International Conference on Fast Sea Transportation, Sydney, 107-113.